

## Article

# Potential Impacts of Industrialization on Coastal Fresh Groundwater Resources in Bangladesh

Mahfuzur R Khan <sup>1,\*</sup>, Fuad Hasan <sup>2</sup>, Majidul Islam <sup>1</sup>, Masuma Chowdhury <sup>1</sup>, Sumiya Sadeak <sup>1</sup>, Al Amin <sup>3</sup>, Farhad Hossain <sup>1</sup> and Kazi Matin Ahmed <sup>1</sup>

<sup>1</sup> Department of Geology, University of Dhaka, Dhaka 1000, Bangladesh; ronysiraji@gmail.com (M.I.); m.chowdhury@du.ac.bd (M.C.); sumiyasadeak2080@gmail.com (S.S.); farhad.geo@du.ac.bd (F.H.); kmahmed@du.ac.bd (K.M.A.)

<sup>2</sup> Mineral Processing Center (MPC), Institute of Mining, Mineralogy, and Metallurgy (IMMM), Bangladesh Council of Scientific and Industrial Research (BCSIR), Joypurhat 5900, Bangladesh; fuad3014@gmail.com

<sup>3</sup> Department of Oceanography and Hydrography, Bangabandhu Sheikh Mujibur Rahman Maritime University, Pallabi, Mirpur-12, Dhaka 1216, Bangladesh; alamin45.geo@gmail.com

\* Correspondence: m.khan@du.ac.bd

**Abstract:** Bangladesh is overly dependent on groundwater and the demand in the near future is expected to increase, as the country is experiencing rapid development and industrial growth. This study assesses the prospect and sustainability of groundwater in Mirsharai Upazila, Chattogram, where a large industrial area, namely ‘Bangabandhu Sheikh Mujib Shilpa Nagar (BSMSN)’, is taking shape. The physical aquifer system was characterized and groundwater quality was mapped. There is one thick aquifer in the northernmost part of the upazila, which splits into three separate aquifers in the south. Water quality indexing suggests that the deep (>130 m) groundwater throughout upazila is good ( $n = 5$ ) to excellent ( $n = 18$ ), while the shallow groundwater is mostly poor to unsuitable for both drinking and irrigation purposes. Because of the close proximity to the sea and the presence of thick clays above the deep freshwater aquifer in the BSMSN area, heavy industrial abstraction poses a threat to the lateral intrusion of seawater and land subsidence. Even a small subsidence in the project area at only a couple of meters above sea level would jeopardize the entire project. This study recommends limiting the use of the deep fresh groundwater for the current population of the upazila.

**Keywords:** groundwater quality; industrialization; water quality index; BSMSN; subsidence; coastal groundwater; Bangladesh



check for updates

**Citation:** Khan, M.R.; Hasan, F.; Islam, M.; Chowdhury, M.; Sadeak, S.; Amin, A.; Hossain, F.; Ahmed, K.M. Potential Impacts of Industrialization on Coastal Fresh Groundwater Resources in Bangladesh.

*Sustainability* **2022**, *14*, 8704.

<https://doi.org/10.3390/su14148704>

Academic Editors: Atiqur Rahman, Shakeel Ahmed, Swapan Talukdar and Abu Reza Md. Towfiqul Islam

Received: 5 June 2022

Accepted: 8 July 2022

Published: 15 July 2022

**Publisher’s Note:** MDPI stays neutral with regard to jurisdictional claims in published maps and institutional affiliations.



**Copyright:** © 2022 by the authors. Licensee MDPI, Basel, Switzerland. This article is an open access article distributed under the terms and conditions of the Creative Commons Attribution (CC BY) license (<https://creativecommons.org/licenses/by/4.0/>).

## 1. Introduction

Groundwater is a major source of the global water supply because it is usually clean, safe, requires little or no treatment, and is less affected by droughts than surface water [1–3]. In south and southeast Asia, it is used extensively for both drinking and irrigation purposes [4,5]. Groundwater degradation, in terms of both quantity and quality, has been a major concern in many countries [6–10]. Although, on a global scale, groundwater withdrawal is less than the available supply [11], there is a large spatial variability [12,13]. Groundwater depletion is particularly evident in heavily irrigated areas across the globe [14–18].

In Bangladesh, groundwater is the major source of freshwater supply for irrigation, industrial, and domestic water supply in both the urban and rural areas [19–22]. However, Bangladesh is one of the worst affected countries in the world for groundwater arsenic [23,24]. An estimated 27.5 million people are chronically exposed to arsenic greater than the WHO guideline value of 10 µg/L through their drinking water [25]. Besides arsenic, groundwater salinity is a major problem in many parts of coastal Bangladesh [20,26,27]. In the coastal area, potable groundwater only exists in aquifers deeper than 150 m, while at shallower depths, most of the water is brackish. Under such

circumstances, it is easier to assume that no local vertical freshwater recharge occurs in the coastal deep aquifer and the only source of freshwater supply it is the deep regional flow [28,29]. However, how far the recharge to the deep aquifer occurs is poorly understood. Understanding the recharge mechanism and recharge area is crucial for managing coastal groundwater, the sole source of potable water for tens of millions of people [28]. Climate-change-induced increased intensity of storm surges and a possible sea level rise poses an additional threat to the management of coastal groundwater in Bangladesh. Away from the coast, extensive irrigation and use of pesticides and other chemicals in the northern part of Bangladesh is deteriorating the groundwater quality [30,31]. Apart from groundwater quality issues, many urban centers and agricultural hubs in the country are experiencing a rapid decline in groundwater levels [21,22], and its impacts are being felt in areas that are tens of kilometers away from the urban center [32–34].

Urbanization and industrialization act as engines for economic growth and social development but also cause environmental degradation, especially in developing countries [35,36]. Increased vulnerability to natural hazards, landscape degradation, groundwater contamination, land surface erosion and reduction, climate change, net productivity reduction etc., are influenced by urbanization and industrialization [37–39]. There is a positive correlation between urbanization (industrialization) and groundwater contamination. Deterioration of both groundwater quality and quantity, in and around many megacities in the world, is evidenced in many studies [32,38,40–44]. Urban and industrial waste are often polluted with dangerous heavy metals such as Cu, Ni, Cd, Cr, As, Pb, and Zn, pathogens and other water contaminants, that eventually find their way into groundwater [45–48] and causes health issues to the consumers [49].

Bangladesh is rapidly transforming from a largely agrarian to an industrialized country. Currently, it is the second largest exporter of readymade garments in the world. Considering the limited land area, high population density, and a large young workforce, industrialization is important for the growth and future of Bangladesh. The contribution of industries to the nation's gross domestic product (GDP) has increased from 19.13% in the 1985–86 fiscal year, to 34.99% in 2020–21 [50]. To keep pace with the fourth industrial revolution, the government of Bangladesh is focusing heavily on the growth of the industrial sector and planning to set up 100 exclusive economic zones in different parts of the country to attract foreign investment by 2030 [50]. Each of these zones will become a high-density industrial center and will promote urbanization around them. It is highly likely that these economic zones will also be hotspots for groundwater contamination. Previously, it is evident that large-scale, unplanned industrial growth has resulted in severe environmental degradation. For example, the tannery industry along the Buriganga River in the capital city of Dhaka, causes severe destruction of the aquatic ecosystem and pollution of the major surface and groundwater sources [51,52].

Although it is understood that groundwater quality deteriorates due to urbanization and industrialization, the exact pathways and timeline of such contamination is poorly understood. This is largely because, in most of the cases, there is no baseline groundwater quality data to compare the post-industrialized water quality. To monitor the evolution of the groundwater quality affected by anthropogenic activities, it is necessary to compile and analyze all the relevant data. The current study area is the largest planned exclusive economic zone in Bangladesh, namely Bangabandhu Sheikh Mujib Shilpa Nagar (BSMSN), which is being implemented by the Bangladesh Economic Zone Authority (BEZA) (Figure 1). More than 580 industries, including garments, automobiles, food, and the chemical industry, are expected to be established there. To run this industrial site every day, approximately 839 million liters/day of freshwater will be required by 2040, which will be collected from nearby surface water sources and groundwater [53,54]. Therefore, this study is focusing on evaluating the spatial variability in hydrogeological and hydrogeochemical parameters in the area that will serve as a baseline paper to assess the impacts of industrialization on water quality in the near future. Besides, this study provides a qualitative assessment of the potential impacts of large-scale groundwater withdrawal in the planned industrial zone on

the water supply of the existing population, as well as the possibility of land subsidence and the overall sustainability of the proposed industrial zone. Furthermore, based on the spatial variation in major ion chemistry, this study provides insights on groundwater flow and the recharge mechanism to deep aquifers in coastal Bangladesh.

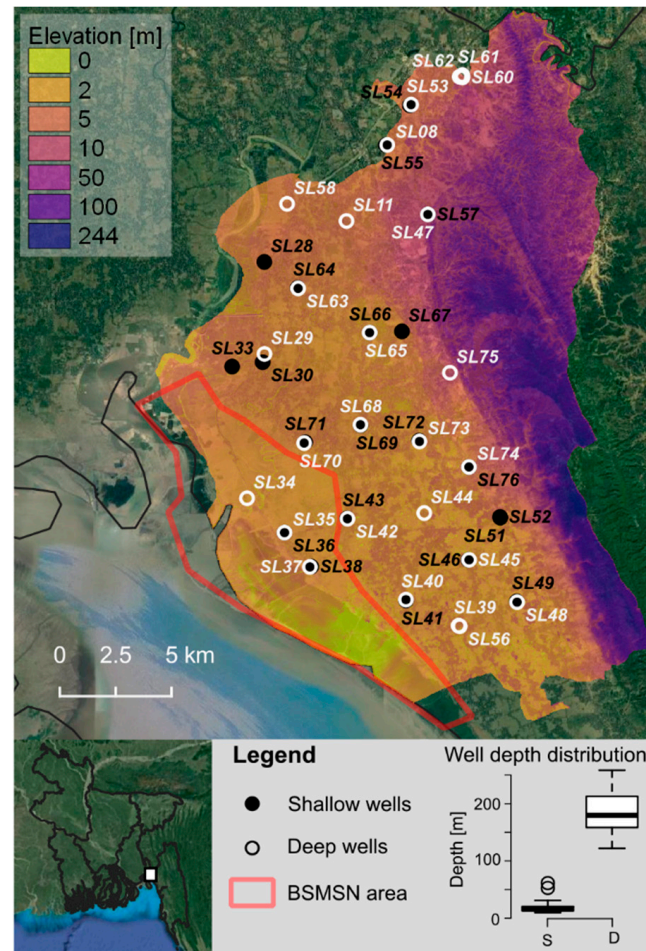


**Figure 1.** Map showing the study area.

### Study Area

The Mirsharai upazila contains both hilly and plain land topography. Our focus is the western part of the upazila, which is a plainland with an elevation between 0 and 10 m. The eastern hilly area has an elevation between 50 and more than 200 m with a very scarce population. The transition from plain land to hills is abrupt and is marked by a regional fault line. The surface geology of the study area has two distinct patterns: the tertiary sediments are exposed in the eastern hilly part and the plainlands are covered with Holocene alluvium and tidal flat sediments along the coast. The northern boundary of the study area is marked by a southerly flowing fresh water river, the Feni river, while the southern boundary is marked by the Bay of Bengal. Mangrove plantations exist along the coastal side in the northwest and southeast parts of the area. In Mirsharai upazila, the total percentage of groundwater use is 95.5% [55]. The study area is located in tropical monsoon and coastal climatic conditions. The study area receives an average of 3000 mm of rainfall per year. The driest month is January receiving an average of 6 mm of rainfall, and the wettest month is July receiving an average of 761 mm of rainfall. The average temperature of the area is 25.7 °C.

## 2. Methods

### 2.1. Aquifer Delineation

Aquifer framework in the study area was delineated based on the interpreted vertical electrical sounding (VES) data at 20 locations and borehole lithological records at five locations (Figure 2b). At each location, borehole lithologies and interpreted VES data were grouped into different layers of aquifers and aquitards based on grain size. Cross-section diagrams were prepared using Rockworks 2017 software to identify the extent and thickness of the aquifer layers (Figure 2).

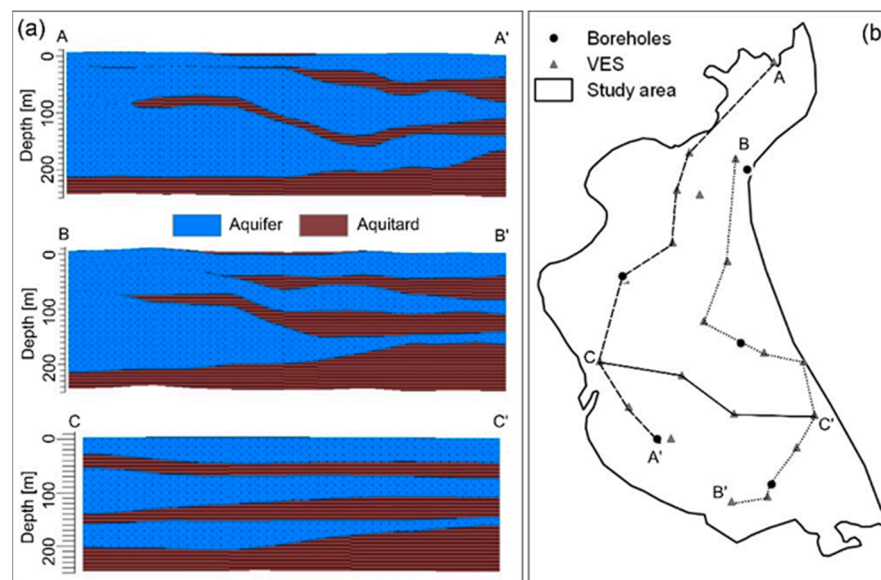


**Figure 2.** Delineation of aquifer geometry based on lithological logs and vertical electrical sounding (VES) data. (a) Cross-section along three different lines in the study area. (b) Map showing the location of the sections, borehole logs, and VES.

### 2.2. Groundwater Sampling

Groundwater samples were collected from a total of 47 sampling sites including 21 shallow (15–60 m depth) and 26 deep (128–260 m depth) wells. PVC bottles of 125 mL were used for water sample collection. Before sampling, each well was purged for 5 to 10 min. Sample bottles were thoroughly washed and water was filtered using a 45 µm micron filter during sampling. Two samples were collected from each location, one was acidified with concentrated HNO<sub>3</sub> for cations and trace elements and the other was non-acidified for anion analysis. Well ID, location, depth, and acidification status were labeled on each sample bottle. The collected samples were transported to the laboratory cautiously and stored in a temperature-controlled environment prior to testing.

### 2.3. Laboratory Analysis

Water samples were analyzed in the Hydro-Geochemistry Laboratory of the Department of Geology, University of Dhaka. The concentration of major cations (Na<sup>+</sup>, K<sup>+</sup>, Ca<sup>2+</sup>, and Mg<sup>2+</sup>) and trace elements (Fe, Mn, As) were measured using atomic absorption spectrometers (AAS). Major anions such as NO<sub>3</sub><sup>-</sup> and SO<sub>4</sub><sup>2-</sup> were analyzed using a UV visible spectrophotometer (410 nm wavelength), while HCO<sub>3</sub><sup>-</sup> and Cl<sup>-</sup> were analyzed using titration methods.

Analytical accuracy was checked for every sample using Equation (1) for ionic balance.

$$\text{Ionic balance (\%)} = [(\Sigma\text{cation} - \Sigma\text{Anions}) / [(\Sigma\text{cation} + \Sigma\text{Anions})] \times 100 \quad (1)$$

All the concentrations of cations and anions were taken in the meq/L unit. If the calculated ionic balance by the above equation was within 5%, the analysis was assumed to be good (Hounslow, 1995); however, a balance up to 10% was accepted in this study.

#### 2.4. Hydrogeochemical Types

Classification of water into distinct hydrogeochemical types provides insights on the geochemical evolution of groundwater and helps identify recharge areas, the ion exchange process, and saline water intrusion. The Chadha index [56], Piper diagram [57], and Durov plot [58] were used for geochemical classification of groundwater in the study area. The Chadha's plot of  $(Ca^{2+} + Mg^{2+})-(Na^{+}+K^{+})$  against  $HCO_3^{-}-(Cl^{-} + SO_4^{2-})$  classifies water into (i) recharge water (Ca-HCO<sub>3</sub> type), (ii) base ion exchange water (Na-HCO<sub>3</sub> type), (iii) reverse ion exchange water (Ca-Mg-Cl type), and (iv) seawater (Na-Cl type). Both the Piper and Durov's classification schemes are based on the plots of major cations ( $Na^{+} + K^{+}$ ,  $Ca^{2+}$ , and  $Mg^{2+}$ ) against major anions ( $HCO_3^{-} + CO_3^{2-}$ ,  $Cl^{-}$ , and  $SO_4^{2-}$ ) in triangular diagrams. In the Piper plot, the cation and anion triangles extend to form a rhombus having 6 distinct water-type zones based on the relative concentration of various ions. Similarly, a square having 8 distinct water type zones is formed in the Durov plot. The position of water samples in various zones of these diagrams indicate the geochemical type as well as geochemical processes.

#### 2.5. Drinking Water Quality (WQI)

Drinking water quality was assessed based on the calculation of a water quality index. The water quality index (WQI) is a quick assessment of suitability of groundwater for drinking purposes, considering the cumulative effects of a number of key water chemistry parameters. Originally developed by Horton [59], WQI is widely used all over the world [60–63]. For the computation of WQI, each of the parameters has been assigned a weight ( $w_i$ ) according to its relative importance in the overall quality of water for drinking purposes (Table 1). A maximum weight of 5 has been assigned to the parameters such as nitrate, total dissolved solids, chloride, arsenic, and fluoride, due to their major importance in water quality assessment and health hazards. A weight of 3 was assigned for  $Mn^{2+}$  and  $SO_4^{2-}$ . For all other parameters, a weight of 2 was considered. Relative weight ( $W_i$ ) was calculated by dividing the weight of individual parameters by the total weight of all parameters. The water quality index for each sample was then calculated by Equation (2).

$$WQI = \sum_{i=1}^n W_i \times \left( \frac{C_i}{S_i} \right) \times 100 \quad (2)$$

In Equation (2),  $W_i$  is the relative weight of each parameter,  $C_i$  is the concentration in the water sample, and  $S_i$  is the Bangladesh drinking water standard for that parameter. Based on the calculated value of WQI, the water samples were classified as excellent ( $WQI < 50$ ), good ( $WQI \geq 50$  to  $<100$ ), poor ( $WQI \geq 100$  to  $<200$ ), very poor ( $WQI \geq 200$  to  $<300$ ), and unacceptable for drinking ( $WQI \geq 300$ ).

#### 2.6. Irrigation Water Quality

Irrigation water quality of each sample was assessed using the Riverside [64] and Wilcox [65] classification schemes. The Riverside classification is based on the sodium absorption ratio (SAR) and electrical conductivity (EC) of the water samples, whereas the Wilcox classification scheme is based on the percentage sodium (%Na) content and EC. Sodium is an important factor for irrigation water quality because sodium reacts with the soil to create sodium hazards by replacing other cations [66]. SAR was calculated by using Equation (3) and % Na was calculated using Equation (4).

$$SAR = \frac{Na^{+}}{\sqrt{\frac{Ca^{2+} + Mg^{2+}}{2}}} \quad (3)$$

$$\%Na = \frac{Na^+}{Ca^{2+} + Mg^{2+} + Na^+ + K^+} \quad (4)$$

**Table 1.** Drinking water quality indexing parameters.

Indexing Parameter	Unit	Standard	Weight ( $w_i$ )	Relative Weight ( $W_i$ )
pH	-	6.5–8.5	2	0.0444
TDS	mg/L	1000	5	0.1111
SO <sub>4</sub> <sup>2-</sup>	mg/L	400	3	0.0667
Cl <sup>-</sup>	mg/L	600	5	0.1111
NO <sub>3</sub> <sup>-</sup>	mg/L	10	5	0.1111
F <sup>-</sup>	mg/L	1	5	0.1111
Ca <sup>2+</sup>	mg/L	75	2	0.0444
Mg <sup>2+</sup>	mg/L	35	2	0.0444
Na <sup>+</sup>	mg/L	200	2	0.0444
K <sup>+</sup>	mg/L	12	2	0.0444
HCO <sub>3</sub> <sup>-</sup>	mg/L	200	2	0.0444
Fe	mg/L	1	2	0.0444
Mn	mg/L	0.1	3	0.0667
As	µg/L	50	5	0.1111
<b>Total</b>			<b>45</b>	<b>1.0000</b>

### 3. Results

#### 3.1. Aquifer Framework

Borehole logs and interpreted VES data suggest that there is one thick aquifer in the northernmost part of the study area, which splits into three separate aquifers in the south (Figure 2). Except for the central part of the study area, the shallowest part of the aquifer is exposed all over the study area below a very thin soil layer. In the central part of the study area, the aquifer lies beneath a 5–7 m thick clay layer. In the south, the second aquifer is 25 to 85 m thick and is separated from the first aquifer by an aquitard of variable thickness. The second aquifer is thickest in the west and thinnest in the east. The third or deep aquifer occurs in the south below approximately 150 m in depth. The aquifer is thinnest in the southeast (20 m) and thickest in the northwest (80 to 120 m). It is separated from the second aquifer by a 30–50 m thick aquitard.

#### 3.2. Groundwater Flow Direction

Groundwater flow direction was determined based on the field measurement of the depth to groundwater level in the monitoring wells. The depth data was later converted to groundwater elevation based on the satellite image. The groundwater level in the shallow aquifer varies between 4 m and 6 m. Though the data are very patchy, some regional trend in flow direction can be deduced from the figure. Generally, the head is higher in the north and northeast than that in the south and southwest. Groundwater flows from the north–northeast to south–southwest direction (Figure 3a). The patchiness in the data is most likely due to inaccurate topography data together with uncertainties in the platform height of the wells. The groundwater level data for the deep aquifer are comparatively more coherent than the shallow data. There is a strong trend in groundwater level, groundwater flows from the NNE to SSW direction (Figure 3b). It is worth noting that, though the flow direction nearly represents the natural condition, the groundwater level may not show an accurate result due to lack of proper elevation data from the field.

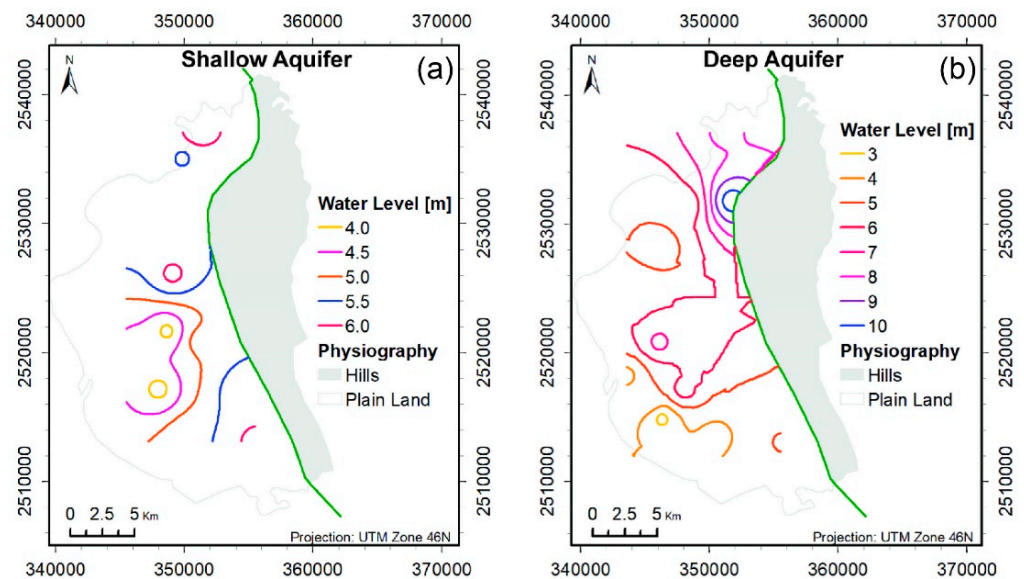


**Figure 3.** Groundwater level contour in the study area of the (a) shallow and (b) deep aquifer.

### 3.3. Physicochemical Characteristics of Groundwater

The pH value of the area ranges from 5.04 to 7.90 with a mean of 6.90, which indicate a slight acidic nature of the groundwater. Moreover, pH values of the 79% studied samples were within the permissible limits suggested by the World Health Organization (WHO) (Table 2). The wells along the Naf river and Bay of Bengal have shown higher EC values than other parts of the area. The groundwater temperature in the study area ranges from 21.5 °C to 29.5 °C in the shallow aquifer and 24.5 °C to 30.5 °C in the deep aquifer. The concentration of the total dissolved solids (TDS) in all groundwater from the deep wells ranges from 64 to 737 mg/L with an average of 443 mg/L. The TDS concentration in the shallow wells ranges from as low as 131 mg/L to as high as >7000 mg/L. Because of the large variation in TDS in the shallow samples, the shallow samples have been divided into two groups: (S1) shallow groundwater with TDS ≤ 1000 mg/L and (S2) shallow groundwater with TDS > 1000 mg/L, for the purpose of statistical analysis and plotting.

The statistical distributions of the concentrations of major cations and anions are summarized in Table 2 and illustrated using box and whisker diagrams for S1, S2, and the deep (D) wells in Figure 4. The overall  $\text{Ca}^{2+}$ ,  $\text{Mg}^{2+}$  and  $\text{Na}^{+}$  concentrations show higher values in the S2 wells compared to the other two categories.  $\text{Na}^{+}$  concentration in the shallow wells (S2 category) shows values higher than the permissible limit by the WHO. The  $\text{K}^{+}$  concentration is higher in both the S1 and S2 categories. The major cation concentration in the deep wells are lower than in the shallow wells. The  $\text{HCO}_3^{-}$  concentrations ranges between 89.25 and 571.88 mg/L with a median concentration of 274.50 mg/L in the S1 wells; 180 to 799.75 mg/L with a median concentration of 588.78 mg/L in the S2 wells; and 45.75 to 533.75 mg/L with a median concentration of 331.69 mg/L in the deep wells. The  $\text{Cl}^{-}$  concentration is higher in the S2 category wells with a median 1047.95 mg/L. The concentration of  $\text{SO}_4^{2-}$  in the shallow and deep wells varies insignificantly, whereas, in the S2 wells, it ranges from 0.20 to 443.80 mg/L with a median value of 53.03 mg/L. The  $\text{NO}_3^{-}$  concentration is generally higher in the S2 wells compared to both the S1 and deep wells. The concentration of  $\text{HCO}_3^{-}$  and  $\text{Na}^{+}$  ions are higher than  $\text{SO}_4^{2-}$   $\text{NO}_3^{-}$  in the groundwater of the area. The major ions are within the permissible limit by the WHO for shallow (S1 category) and deep wells, except the S2 category shallow wells.

**Table 2.** Statistical distribution of the water quality parameters.

Parameters	Min	Max	Mean	SD	WHO Guidelines
Temperature	21.5	30.5	26.5	3.7	-
pH	5.04	7.90	6.90	0.57	6.5–9.2
EC ( $\mu\text{S}/\text{cm}$ ), 25 °C	60	9540	1628	2086	-
Eh (mV)	−167	−195	−52	−83	850
TDS (mg/L)	65	7114	1126	1359	1000
Sodium (mg/L)	2.10	1748	236.4	340.5	200
Potassium (mg/L)	0.62	20.19	4.95	4.70	200
Calcium (mg/L)	5.44	171.7	28.48	30.58	200
Magnesium (mg/L)	6.67	280.1	50.83	57.59	150
Bicarbonate (mg/L)	45.75	799.8	375.0	195.6	125–350
Chloride (mg/L)	1.38	3720	393.3	755.8	250
Nitrate (mg/L)	0.07	13.35	2.64	3.01	50
Sulphate (mg/L)	0.11	443.8	29.6	78.4	250
Manganese (mg/L)	<DL	2.45	0.25	0.40	0.1
Iron (mg/L)	0.05	10.14	2.34	2.60	0.3
Fluoride (mg/L)	<DL	0.65	0.28	0.15	1.5
Bromide (mg/L)	<DL	17.3	1.37	3.09	-
Phosphate (mg/L)	<DL	9.80	0.97	1.97	0.3
Nitrite (mg/L)	<DL	0.42	0.04	0.09	0.5
Arsenic ( $\mu\text{g}/\text{L}$ )	<DL	1000	131.3	213.2	10
Hardness	41	1501	280	308	-
%Na	8.12	83.41	51.59	20.39	-
SAR	0.13	19.62	5.07	4.85	-

>DL Less than the detection limit

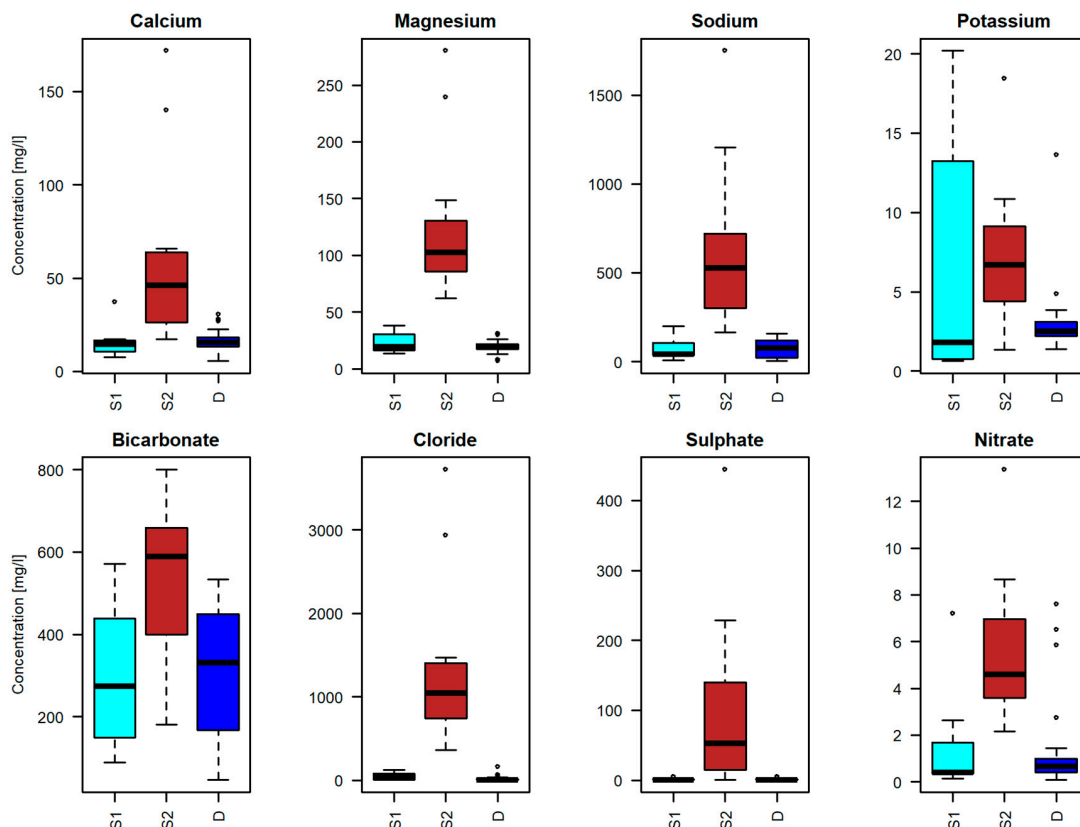


**Figure 4.** Statistical distribution of major ions among three groups of samples; (S1) shallow groundwater with TDS  $\leq$  1000 mg/L, (S2) shallow groundwater with TDS  $>$  1000 mg/L, and (D) deep groundwater.

The statistical distributions of the concentrations of minor constituents and trace elements are summarized in Table 2 and illustrated using box and whisker diagrams for S1, S2, and the deep (D) wells in Figure 5. The concentration of the trace/minor constituents among three groups of samples are identical with the distribution of the major ion concentration. The S2 category shallow wells show higher values than the other S1 shallow and deep wells. The median concentration of manganese is 0.20, 0.38, and 0.03 mg/L for the S1, S2, and deep wells, respectively. The ranges of concentrations in the S1 and deep wells are similar, while those in S2 wells vary considerably. The median concentration of iron is 1.93, 2.36, and 0.46 mg/L for the S1, S2, and deep wells, respectively. However, there is a wide variation in the iron concentration in all three categories of wells. The median concentration of bromide in the S1 and deep wells are similar, while that in S2 wells varies considerably. It ranges from 0 to 0.54 mg/L in the S1 wells, 0 to 17.30 mg/L in the S2 wells, and nil to 0.46 mg/L in the deep wells. The concentration of fluoride and phosphate are significantly higher in the shallow S2 wells than the S1 shallow and deep wells. Moreover, the manganese, iron, and phosphate concentrations are higher than the WHO limit in groundwater, whereas the fluoride and bromide are within that limit.

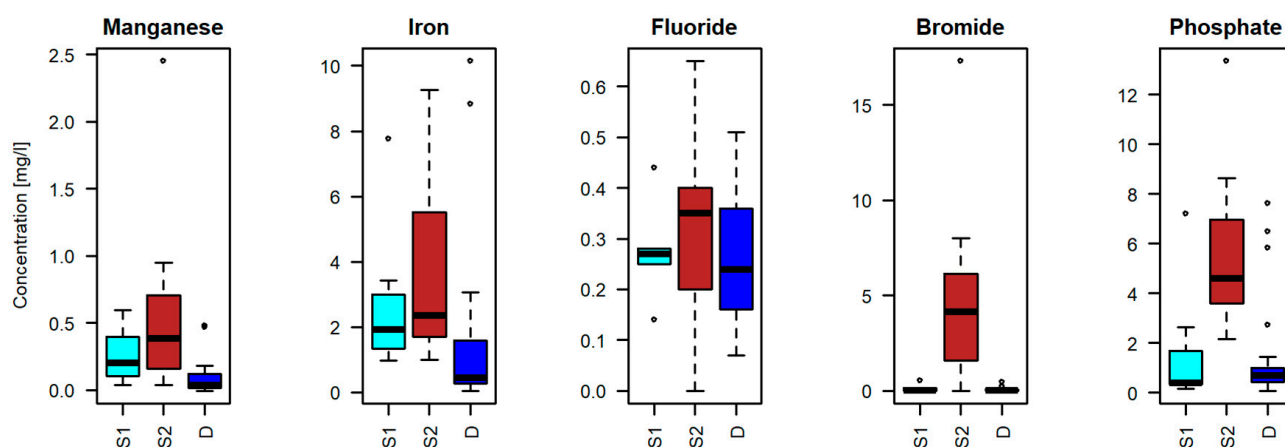


**Figure 5.** Statistical distribution of trace/minor constituents among three groups of samples; (S1) shallow groundwater with TDS  $\leq 1000$  mg/L, (S2) shallow groundwater with TDS  $> 1000$  mg/L, and (D) deep groundwater.

### 3.4. Hydrogeochemical Types

Except for only one sample, all deep groundwater samples fall in either the recharge or base ion exchange quadrants on the Chadha's plot (Figure 6a); this is also supported by the Piper (Figure 6d) and Durov's plots (Figure 6e). The spatial distribution of Chadha's index reveals that the recharging to the deep aquifer occurs in the northern half of the study area (Ca-HCO<sub>3</sub> type), whereas base ion exchange occurs down the groundwater flow paths in the southern half of the study area, where the water becomes Na-HCO<sub>3</sub> type (Figure 6b). The exception is a 207 m deep well located in the north central part of the study area that exhibits a reverse ion exchange signature (Ca-Mg-Cl type) (Figure 6). In contrast, except for one shallow well, all samples have TDS  $> 1000$  mg/L falls in the seawater (Na-Cl type) class on the Chadha's plot (Figure 6a), Na-Cl-SO<sub>4</sub> type in the Piper diagram (Figure 6d), and on the seawater mixing lines in the Durov plot (Figure 6e). The exception is located in the central part of the study area and exhibits characteristics of reverse ion exchange (Ca-Mg-Cl type) processes. The remaining shallow wells with TDS  $< 1000$  mg/L show a similar water chemistry to the deep groundwater, i.e., they are either recharging water (Ca-HCO<sub>3</sub> type) or modified by a base ion exchange where calcium is replaced by sodium ions. These wells are located in the north and eastern margins near the hills (Figure 6b).

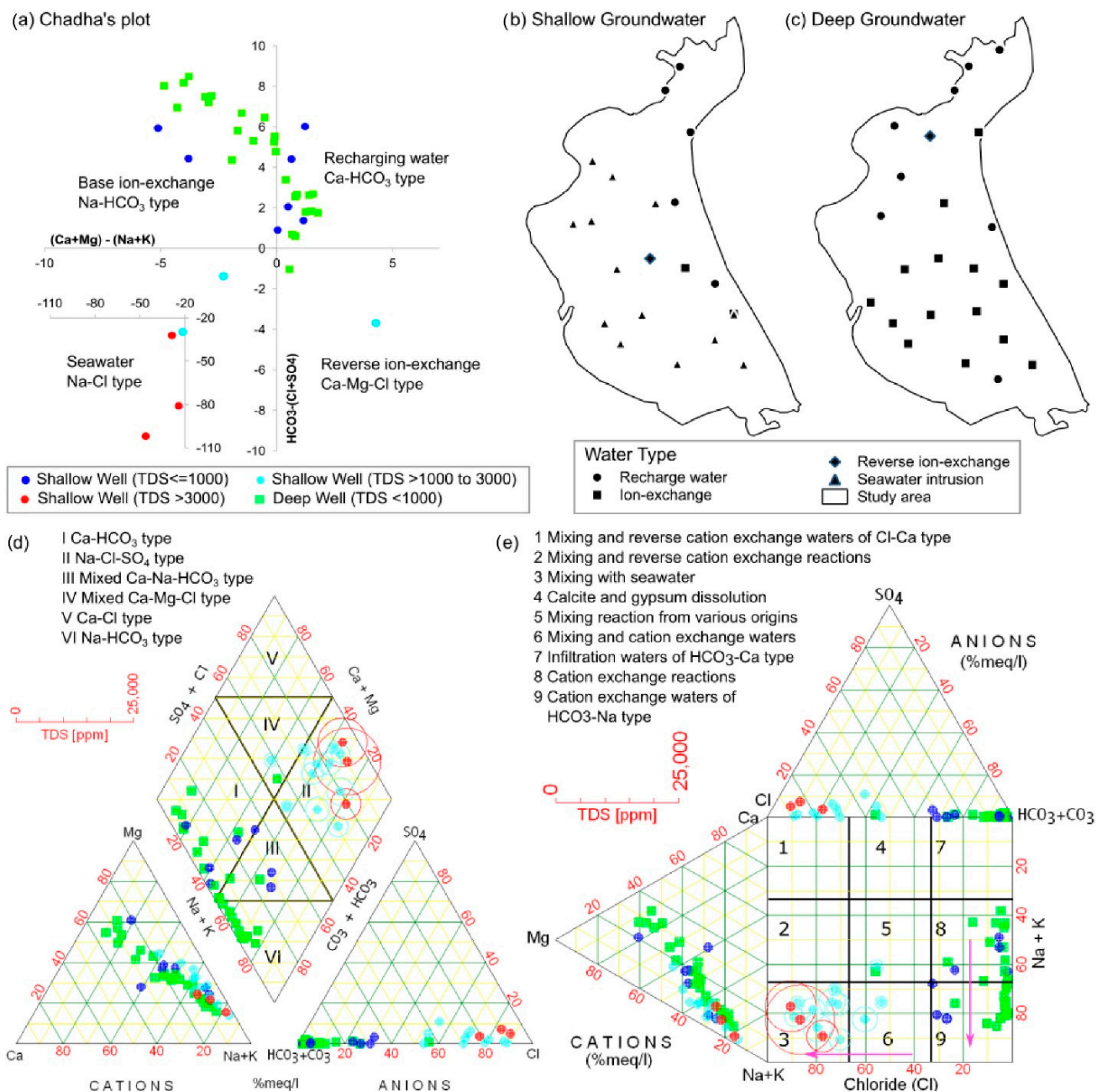


**Figure 6.** Graphical plots depicting various water types and geochemical processes in the study area. (a) Chadha's plot of  $(Ca + Mg) - (Na + K)$  against  $HCO_3 - (Cl + SO_4)$  for identifying water type in the study area. (b,c) Spatial distribution of Chadha's index for shallow groundwater and deep groundwater, respectively. (d,e) Piper and Durov plots, respectively.

### 3.5. Drinking Water Quality Index

The calculated drinking water quality index shows that all 26 deep wells have excellent ( $n = 20$ ) to good ( $n = 6$ ) water quality, whereas only three out of the 21 shallow wells have excellent ( $n = 2$ ) to good ( $n = 1$ ) water quality (Table 3). A total of 15 shallow wells have poor ( $n = 8$ ) to very poor ( $n = 7$ ) drinking water quality, and water in the remaining three shallow wells are unsuitable for drinking (Table 3). Excellent quality deep groundwater is distributed throughout the study area with sporadic pocket areas of good quality water (Figure 7b). In contrast, the excellent and good quality shallow groundwater exists only in the north and in the east, along the boundary of the hills (Figure 7a).

**Table 3.** Calculated groundwater quality index of the shallow and deep wells.

Groundwater Quality Range	Groundwater Quality	No. of Shallow Wells	No. of Deep Wells
<50	Excellent	2	20
50–100	Good	1	6
100–200	Poor	8	-
200–300	Very poor	7	-
>300	Unsuitable for drinking	3	-

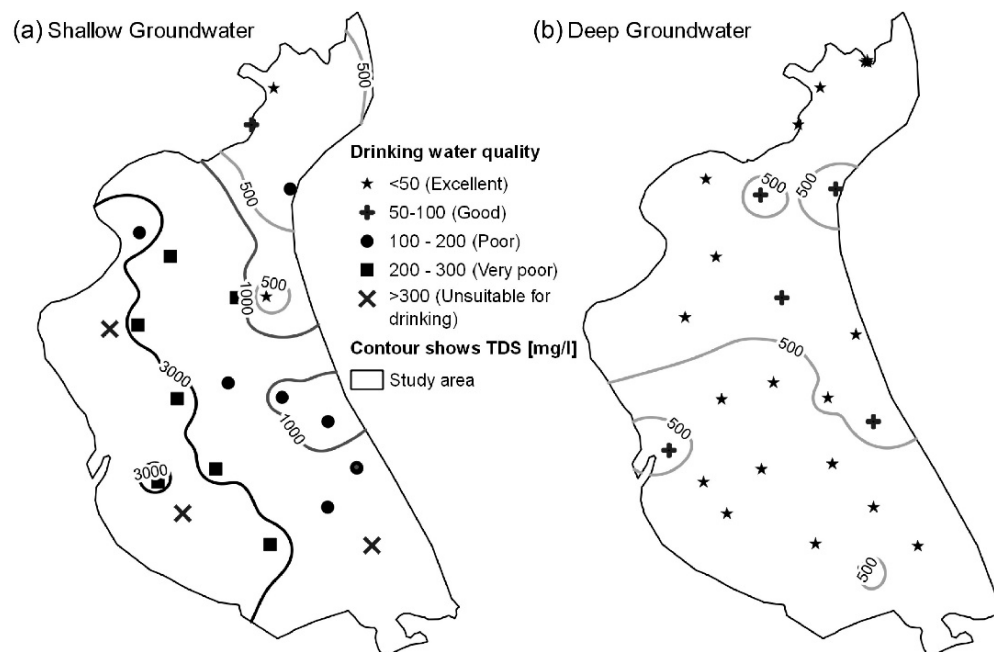


**Figure 7.** Spatial distribution of drinking water quality index of (a) shallow and (b) deep groundwater.

### 3.6. Irrigation Water Quality

Shallow groundwater with TDS > 1000 mg/L has medium to high SAR and EC > 2000  $\mu$ S/cm, indicating a risk of alkali and salinity hazard if this water is used for irrigation (Figure 8a,c). In contrast, deep groundwater throughout the study area and most of the northern shallow groundwater with TDS < 1000 mg/L has low SAR and conductivity <750  $\mu$ S/cm (Figure 8a,c,d). The Wilcox plot also shows the same pattern as the Riverside classification scheme. All deep wells and shallow wells (TDS  $\leq$  1000 mg/L) are falling in the excellent to good, and permissible to doubtful classes, whereas the shallow wells (TDS > 1000 mg/L) are predominantly doubtful and unsuitable for agricultural purposes (Figure 8b,e,f).

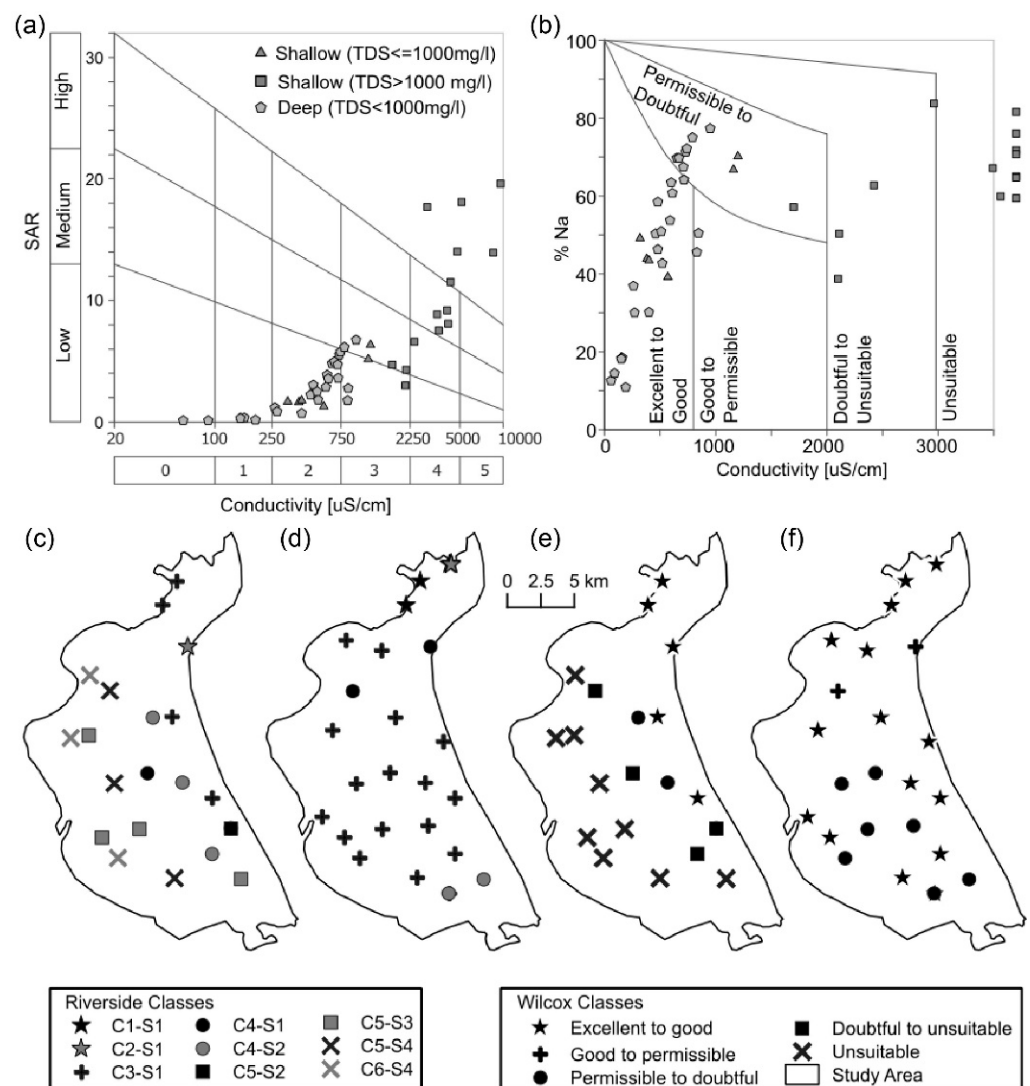


**Figure 8.** (a) Riverside classification of irrigation water, (b) Wilcox classification of irrigation water. Map showing spatial distribution of Riverside (c,d) and Wilcox (e,f) classes for shallow (c,e) and deep (d,f) groundwater, respectively.

## 4. Discussion

### 4.1. Groundwater Sustainability for Industrial Abstraction

The half a million people living in Mirsharai upazila entirely depend on groundwater for drinking, while irrigation is mostly based on surface water. In the northern part of the upazila, people install their wells at both a shallow and deeper depth, while in the southern part, all wells are deep because of the salinity of the shallow aquifer. Groundwater quality assessment indicates that the deep groundwater is suitable for both drinking and irrigation, while the shallow groundwater is unsuitable for either use in most parts of the study area, except in the north. Major ion chemistry and their various indices indicate that recharges to the deep aquifer occur in a small area in the north and flow southward, where the deep aquifer is confined in nature. Therefore, a large-scale abstraction of the deep groundwater in the planned industrial area, which is more than 15 km south of the recharge area, would likely cause a rapid depletion of the head in the deep aquifer. The proposed economic zone is along the coastline in the southwest. Hence, even a small drop in hydraulic head in the confined deep aquifer within the economic zone is likely to impact the area in several ways. First, a drop in head in the deep aquifer near the coastline would induce landward migration of the seawater–freshwater interface in the deep aquifer. However, the time it

would take to reach the project area will depend on the magnitude of the head drop and the current position of the seawater–freshwater in the deep system. Second, a large drop in head in the deep system in the project area will induce the vertical migration of salty water from a shallow depth through the overlying mud layers. Third, the release of water from overlying clays will induce land subsidence. Perhaps this is the most important concern about large-scale abstraction within the industrial zone. The land surface elevation within the project area is one or two meters above sea level. Therefore, even a small subsidence would jeopardize the entire project.

#### 4.2. Implications of Groundwater Chemistry to Flow System

The spatial and depth distribution of groundwater chemistry reveals some important features of the groundwater flow system in the study area. There seems to be a separate shallow and deep groundwater system in the southern part of the study area. While in the northern part of the area, where there is no aquitard separating these two aquifers, their groundwater chemistry is identical. Moreover, this is also the recharge area for both the aquifers. The shallow aquifers also seem to get recharged along the eastern boundary hills. The TDS contour in the shallow system (Figure 7a) exhibits a systematic increase in TDS in the SW direction towards the sea, down the topographic gradient. This pattern salinization in the shallow system could be due to lateral intrusion of seawater from the Bay of Bengal or due to periodic inundation of land areas due to storm surge and vertical infiltration across the land surface. The latter is more likely because the lateral intrusion model cannot explain the lack of salinity in the deep system. The shallow and deep systems are completely isolated in areas where the shallow system is brackish (Figure 2), and this could be the reason why vertical infiltration did not occur in the deep system.

The observed pattern of salinity distribution in the groundwater is also consistent throughout southern coastal Bangladesh, but on a much larger spatial scale because of the geological and topographic configurations. Generally, in south–central coastal Bangladesh, brackish water is found at a shallower depth, up to a landward distance of >100 km from the coastline [28]. Occurrences of brackish water at a shallow depth and freshwater at a deeper depth testify that the deep groundwater has a recharge location hundreds of kilometers away from the coastline [28]. In the current study area, the brackish water at a shallow depth is confined within only 15 km of landward distance from the coastline and the recharge area for the deep groundwater is only a few tens of kilometers away from the coastline. The deep groundwater is fresh, even near the coastline where the land surface is flat, with an elevation of only a meter above sea level. This indicates that the deep fresh groundwater may even exist in the offshore region; this seaward extension is either due to aquifer heterogeneity [67,68] or is related to the sea level regression 18,000 years ago [29,69,70], or both. A modeling study [71] indicated that deep fresh groundwater that extended tens of kilometers in the seaward direction during the last glacial maximum, when the sea level dropped by more than 100 m, has not yet reached an equilibrium with the sea level rise over the last 18,000 years [71]. In any case, the position of the seawater–freshwater interface in the deep aquifer is currently unknown. Therefore, it is currently futile to quantify the timeframe of pumping-induced lateral encroachment of seawater in to the deep aquifer.

## 5. Conclusions

This study recommends limiting the use of the deep fresh groundwater for the current population of the upazila. This is because heavy industrial abstraction is likely to cause lateral intrusion of seawater in the deep aquifer and land subsidence over the entire economic zone area. The timeline of the lateral intrusion of seawater depends on the current position of the seawater–freshwater interface in the deep aquifer, which is currently unknown and perhaps located several kilometers offshore. Depending on the pumping intensity and distance of the interface, it may take decades to reach the area, since the movement of the interface is slow. However, because of the presence of thick, soft marine

clays above and below the deep confined aquifer, pumping-induced subsidence of the order of a meter or so would be immediate. Since the elevation in the project area is only a couple of meters above sea level, such subsidence would jeopardize the entire project. A modeling study is suggested to quantify the probable subsidence for various scenarios of groundwater abstraction in the proposed industrial area. Should there be no heavy industrial abstraction, the existing fresh groundwater in the deep aquifer can sustainably supply drinking water to the existing population of Mirsharai Upazila.

**Author Contributions:** Conceptualization, M.R.K.; methodology, M.R.K.; software, M.R.K. and M.C.; validation, M.R.K. and K.M.A.; formal analysis, F.H. (Fuad Hasan), M.I. and A.A.; investigation, F.H. (Fuad Hasan) and K.M.A.; resources, M.R.K., K.M.A. and F.H. (Fuad Hasan); data curation, F.H. (Fuad Hasan), M.I. and A.A.; writing—original draft preparation, M.R.K., M.C., S.S. and F.H. (Farhad Hossain); writing—review and editing, K.M.A., F.H. (Fuad Hasan), M.I. and A.A.; visualization, S.S. and F.H. (Farhad Hossain); supervision, K.M.A. All authors have read and agreed to the published version of the manuscript.

**Funding:** This research received no external funding and The APC was partially funded by the University of Dhaka.

**Institutional Review Board Statement:** Not applicable.

**Informed Consent Statement:** Not applicable.

**Data Availability Statement:** Data provided in the ref [72].

**Acknowledgments:** The authors would like to thank the “Urban Development Directorate” for their continuous support during data collection. We are pleased to acknowledge the department of Geology, University of Dhaka, for providing us with the laboratory amenities for water chemistry analysis.

**Conflicts of Interest:** The author declares no conflict of interest.

## References

1. Fiinen, M.N.; Arshad, M. The International Scale of the Groundwater Issue. In *Integrated Groundwater Management*; Springer International Publishing: Cham, Switzerland, 2016; pp. 21–48.
2. Giordano, M. Global Groundwater? Issues and Solutions. *Annu. Rev. Environ. Resour.* **2009**, *34*, 153–178. [[CrossRef](#)]
3. Taylor, R.G.; Scanlon, B.; Döll, P.; Rodell, M.; van Beek, R.; Wada, Y.; Longuevergne, L.; Leblanc, M.; Famiglietti, J.S.; Edmunds, M.; et al. Ground Water and Climate Change. *Nat. Clim. Chang.* **2013**, *3*, 322–329. [[CrossRef](#)]
4. Lutz, A.F.; Immerzeel, W.W.; Siderius, C.; Wijngaard, R.R.; Nepal, S.; Shrestha, A.B.; Wester, P.; Biemans, H. South Asian Agriculture Increasingly Dependent on Meltwater and Groundwater. *Nat. Clim. Chang.* **2022**, *12*, 566–573. [[CrossRef](#)]
5. Siebert, S.; Burke, J.; Faures, J.M.; Frenken, K.; Hoogeveen, J.; Döll, P.; Portmann, F.T. Groundwater Use for Irrigation—A Global Inventory. *Hydrol. Earth Syst. Sci.* **2010**, *14*, 1863–1880. [[CrossRef](#)]
6. Berg, M.; Stengel, C.; Trang, P.; Hungviet, P.; Sampson, M.; Leng, M.; Samreth, S.; Fredericks, D. Magnitude of Arsenic Pollution in the Mekong and Red River Deltas—Cambodia and Vietnam. *Sci. Total Environ.* **2007**, *372*, 413–425. [[CrossRef](#)]
7. Fendorf, S.; Michael, H.A.; van Geen, A. Spatial and Temporal Variations of Groundwater Arsenic in South and Southeast Asia. *Science* **2010**, *328*, 1123–1127. [[CrossRef](#)] [[PubMed](#)]
8. Famiglietti, J.S. The Global Groundwater Crisis. *Nat. Clim. Chang.* **2014**, *4*, 945–948. [[CrossRef](#)]
9. Hartmann, A.; Jasechko, S.; Gleeson, T.; Wada, Y.; Andreo, B.; Barberá, J.A.; Brielmann, H.; Bouchaou, L.; Charlier, J.-B.; Darling, W.G.; et al. Risk of Groundwater Contamination Widely Underestimated Because of Fast Flow into Aquifers. *Proc. Natl. Acad. Sci. USA* **2021**, *118*, e2024492118. [[CrossRef](#)]
10. Brammer, H.; Ravenscroft, P. Arsenic in Groundwater: A Threat to Sustainable Agriculture in South and South-East Asia. *Environ. Int.* **2009**, *35*, 647–654. [[CrossRef](#)]
11. Hanasaki, N.; Yoshikawa, S.; Pokhrel, Y.; Kanae, S. A Global Hydrological Simulation to Specify the Sources of Water Used by Humans. *Hydrol. Earth Syst. Sci.* **2018**, *22*, 789–817. [[CrossRef](#)]
12. Alley, W.M.; Healy, R.W.; LaBaugh, J.W.; Reilly, T.E. Flow and Storage in Groundwater Systems. *Science* **2002**, *296*, 1985–1990. [[CrossRef](#)] [[PubMed](#)]
13. Waibel, M.S.; Gannett, M.W.; Chang, H.; Hulbe, C.L. Spatial Variability of the Response to Climate Change in Regional Groundwater Systems—Examples from Simulations in the Deschutes Basin, Oregon. *J. Hydrol.* **2013**, *486*, 187–201. [[CrossRef](#)]
14. Wada, Y.; van Beek, L.P.H.; van Kempen, C.M.; Reckman, J.W.T.M.; Vasak, S.; Bierkens, M.F.P. Global Depletion of Groundwater Resources. *Geophys. Res. Lett.* **2010**, *37*, L20402. [[CrossRef](#)]

15. Döll, P.; Müller Schmied, H.; Schuh, C.; Portmann, F.T.; Eicker, A. Global-Scale Assessment of Groundwater Depletion and Related Groundwater Abstractions: Combining Hydrological Modeling with Information from Well Observations and GRACE Satellites. *Water Resour. Res.* **2014**, *50*, 5698–5720. [[CrossRef](#)]
16. Konikow, L.F.; Kendy, E. Groundwater Depletion: A Global Problem. *Hydrogeol. J.* **2005**, *13*, 317–320. [[CrossRef](#)]
17. Carrard, N.; Foster, T.; Willetts, J. Groundwater as a Source of Drinking Water in Southeast Asia and the Pacific: A Multi-Country Review of Current Reliance and Resource Concerns. *Water* **2019**, *11*, 1605. [[CrossRef](#)]
18. Chang, Y.-J.; Zhu, D. Water Security of the Megacities in the Yangtze River Basin: Comparative Assessment and Policy Implications. *J. Clean. Prod.* **2021**, *290*, 125812. [[CrossRef](#)]
19. Shamsudduha, M.; Taylor, R.G.; Ahmed, K.M.; Zahid, A. The Impact of Intensive Groundwater Abstraction on Recharge to a Shallow Regional Aquifer System: Evidence from Bangladesh. *Hydrogeol. J.* **2011**, *19*, 901–916. [[CrossRef](#)]
20. Shamsudduha, M.; Joseph, G.; Haque, S.S.; Khan, M.R.; Zahid, A.; Ahmed, K.M.U. Multi-Hazard Groundwater Risks to Water Supply from Shallow Depths: Challenges to Achieving the Sustainable Development Goals in Bangladesh. *Expo. Health* **2020**, *12*, 657–670. [[CrossRef](#)]
21. Hoque, M.A.; Hoque, M.M.; Ahmed, K.M. Declining Groundwater Level and Aquifer Dewatering in Dhaka Metropolitan Area, Bangladesh: Causes and Quantification. *Hydrogeol. J.* **2007**, *15*, 1523–1534. [[CrossRef](#)]
22. Moshfika, M.; Biswas, S.; Mondal, M.S. Assessing Groundwater Level Declination in Dhaka City and Identifying Adaptation Options for Sustainable Water Supply. *Sustainability* **2022**, *14*, 1518. [[CrossRef](#)]
23. Alam, M.G.M.; Allinson, G.; Stagnitti, F.; Tanaka, A.; Westbrooke, M. Arsenic Contamination in Bangladesh Groundwater: A Major Environmental and Social Disaster. *Int. J. Environ. Health Res.* **2002**, *12*, 235–253. [[CrossRef](#)] [[PubMed](#)]
24. Neumann, R.B.; Ashfaq, K.N.; Badruzzaman, A.B.M.; Ashraf Ali, M.; Shoemaker, J.K.; Harvey, C.F. Anthropogenic Influences on Groundwater Arsenic Concentrations in Bangladesh. *Nat. Geosci.* **2010**, *3*, 46–52. [[CrossRef](#)]
25. Charles, K.J.; Ong, L.A.; Achi, N.E.; Ahmed, K.M.; Khan, M.R. Bangladesh MICS 2019: Water Quality Thematic Report; Dhaka, 2021. Available online: <https://psb.gov.bd/policies/wqtr2019.pdf> (accessed on 5 June 2022).
26. Ayers, J.C.; Goodbred, S.; George, G.; Fry, D.; Benneyworth, L.; Hornberger, G.; Roy, K.; Karim, M.R.; Akter, F. Sources of Salinity and Arsenic in Groundwater in Southwest Bangladesh. *Geochem. Trans.* **2016**, *17*, 4. [[CrossRef](#)] [[PubMed](#)]
27. Salehin, M.; Chowdhury, M.M.A.; Clarke, D.; Mondal, S.; Nowreen, S.; Jahiruddin, M.; Haque, A. Mechanisms and Drivers of Soil Salinity in Coastal Bangladesh. In *Ecosystem Services for Well-Being in Deltas*; Springer International Publishing: Cham, Switzerland, 2018; pp. 333–347.
28. Ravenscroft, P.; McArthur, J.M.; Hoque, M.A. Stable Groundwater Quality in Deep Aquifers of Southern Bangladesh: The Case against Sustainable Abstraction. *Sci. Total Environ.* **2013**, *454–455*, 627–638. [[CrossRef](#)] [[PubMed](#)]
29. Aggarwal, P.K.; Froehlich, K.; Basu, A.R.; Poreda, R.J.; Kulkarni, K.M.; Tarafdar, S.A.; Ali, M.; Ahmed, N.; Hussain, A.; Rahman, M.; et al. *A Report on Isotope Hydrology of Groundwater in Bangladesh: Implications for Characterization and Mitigation of Arsenic in Groundwater*; INIS-XA-648; International Atomic Energy Agency, Department of Technical Co-operation: Vienna, Austria, 2000.
30. Salman, S.A.; Shahid, S.; Mohsenipour, M.; Asgari, H. Impact of Landuse on Groundwater Quality of Bangladesh. *Sustain. Water Resour. Manag.* **2018**, *4*, 1031–1036. [[CrossRef](#)]
31. Haque, S.E. An Overview of Groundwater Quality in Bangladesh. In *Groundwater of South Asia*; Mukherjee, A., Ed.; Springer: Singapore, 2018; pp. 205–232.
32. Khan, M.R.; Koneshloo, M.; Knappett, P.S.K.; Ahmed, K.M.; Bostick, B.C.; Mailloux, B.J.; Mozumder, R.H.; Zahid, A.; Harvey, C.F.; Van Geen, A.; et al. Megacity Pumping and Preferential Flow Threaten Groundwater Quality. *Nat. Commun.* **2016**, *7*, 12833. [[CrossRef](#)]
33. Knappett, P.S.K.; Mailloux, B.J.; Choudhury, I.; Khan, M.R.; Michael, H.A.; Barua, S.; Mondal, D.R.; Steckler, M.S.; Akhter, S.H.; Ahmed, K.M.; et al. Vulnerability of Low-Arsenic Aquifers to Municipal Pumping in Bangladesh. *J. Hydrol.* **2016**, *539*, 674–686. [[CrossRef](#)]
34. Mozumder, M.R.H.; Michael, H.A.; Mihajlov, I.; Khan, M.R.; Knappett, P.S.K.; Bostick, B.C.; Mailloux, B.J.; Ahmed, K.M.; Choudhury, I.; Koffman, T.; et al. Origin of Groundwater Arsenic in a Rural Pleistocene Aquifer in Bangladesh Depressurized by Distal Municipal Pumping. *Water Resour. Res.* **2020**, *56*, e2020WR027178. [[CrossRef](#)]
35. Azam, M.; Khan, A.Q. Urbanization and Environmental Degradation: Evidence from Four SAARC Countries—Bangladesh, India, Pakistan, and Sri Lanka. *Environ. Prog. Sustain. Energy* **2016**, *35*, 823–832. [[CrossRef](#)]
36. Capps, K.A.; Bentsen, C.N.; Ramirez, A. Poverty, Urbanization, and Environmental Degradation: Urban Streams in the Developing World. *Freshw. Sci.* **2015**, *35*, 429–435. [[CrossRef](#)]
37. Lu, Q.; Gao, Z.; Ning, J.; Bi, X.; Wang, Q. Impact of Progressive Urbanization and Changing Cropping Systems on Soil Erosion and Net Primary Production. *Ecol. Eng.* **2015**, *75*, 187–194. [[CrossRef](#)]
38. Onodera, S. Subsurface Pollution in Asian Megacities. In *Groundwater and Subsurface Environments*; Springer: Tokyo, Japan, 2011; pp. 159–184.
39. Wenzel, F.; Bendimerad, F.; Sinha, R. Megacities—Megarisks. *Nat. Hazards* **2007**, *42*, 481–491. [[CrossRef](#)]
40. Bodrud-Doza, M.; Islam, S.M.D.-U.; Rume, T.; Quraishi, S.B.; Rahman, M.S.; Bhuiyan, M.A.H. Groundwater Quality and Human Health Risk Assessment for Safe and Sustainable Water Supply of Dhaka City Dwellers in Bangladesh. *Groundw. Sustain. Dev.* **2020**, *10*, 100374. [[CrossRef](#)]

41. Haque, S.J.; Onodera, S.; Shimizu, Y. An Overview of the Effects of Urbanization on the Quantity and Quality of Groundwater in South Asian Megacities. *Limnology* **2013**, *14*, 135–145. [[CrossRef](#)]
42. Umezawa, Y.; Hosono, T.; Onodera, S.; Siringan, F.; Buapeng, S.; Delinom, R.; Yoshimizu, C.; Tayasu, I.; Nagata, T.; Taniguchi, M. Sources of Nitrate and Ammonium Contamination in Groundwater under Developing Asian Megacities. *Sci. Total Environ.* **2008**, *404*, 361–376. [[CrossRef](#)]
43. Onodera, S.; Saito, M.; Sawano, M.; Hosono, T.; Taniguchi, M.; Shimada, J.; Umezawa, Y.; Lubis, R.F.; Buapeng, S.; Delinom, R. Effects of Intensive Urbanization on the Intrusion of Shallow Groundwater into Deep Groundwater: Examples from Bangkok and Jakarta. *Sci. Total Environ.* **2008**, *404*, 401–410. [[CrossRef](#)] [[PubMed](#)]
44. Ramos Leal, J.A.; Noyola Medrano, C.; Tapia Silva, F.O. Aquifer Vulnerability and Groundwater Quality in Mega Cities: Case of the Mexico Basin. *Environ. Earth Sci.* **2010**, *61*, 1309–1320. [[CrossRef](#)]
45. Khatri, N.; Tyagi, S. Influences of Natural and Anthropogenic Factors on Surface and Groundwater Quality in Rural and Urban Areas. *Front. Life Sci.* **2015**, *8*, 23–39. [[CrossRef](#)]
46. Opoku, P.A.; Anornu, G.K.; Gibrilla, A.; Owusu-Ansah, E.d.-G.J.; Ganyaglo, S.Y.; Egbi, C.D. Spatial Distributions and Probabilistic Risk Assessment of Exposure to Heavy Metals in Groundwater in a Peri-Urban Settlement: Case Study of Atonsu-Kumasi, Ghana. *Groundw. Sustain. Dev.* **2020**, *10*, 100327. [[CrossRef](#)]
47. Bhutiani, R.; Kulkarni, D.B.; Khanna, D.R.; Gautam, A. Water Quality, Pollution Source Apportionment and Health Risk Assessment of Heavy Metals in Groundwater of an Industrial Area in North India. *Expo. Health* **2016**, *8*, 3–18. [[CrossRef](#)]
48. Rahman, M.A.T.M.T.; Paul, M.; Bhoumik, N.; Hassan, M.; Alam, M.K.; Aktar, Z. Heavy Metal Pollution Assessment in the Groundwater of the Meghna Ghat Industrial Area, Bangladesh, by Using Water Pollution Indices Approach. *Appl. Water Sci.* **2020**, *10*, 186. [[CrossRef](#)]
49. Jaishankar, M.; Tseten, T.; Anbalagan, N.; Mathew, B.B.; Beeregowda, K.N. Toxicity, Mechanism and Health Effects of Some Heavy Metals. *Interdiscip. Toxicol.* **2014**, *7*, 60–72. [[CrossRef](#)]
50. GoB. *Bangladesh Economic Review 2021*; GoB: Dhaka, Bangladesh, 2021.
51. Whitehead, P.G.; Bussi, G.; Peters, R.; Hossain, M.A.; Softley, L.; Shawal, S.; Jin, L.; Rampley, C.P.N.; Holdship, P.; Hope, R.; et al. Modelling Heavy Metals in the Buriganga River System, Dhaka, Bangladesh: Impacts of Tannery Pollution Control. *Sci. Total Environ.* **2019**, *697*, 134090. [[CrossRef](#)] [[PubMed](#)]
52. Alam, M.S.; Han, B.; Al-Mizan; Pichtel, J. Assessment of Soil and Groundwater Contamination at a Former Tannery District in Dhaka, Bangladesh. *Environ. Geochem. Health* **2020**, *42*, 1905–1920. [[CrossRef](#)]
53. BEZA. *Bangabandhu Sheikh Mujib Shilpanagar, Mirsarai-Sitakundu-Sonagazi, Chattogram-Feni*; Prime Minister’s Office: Dhaka, Bangladesh, 2020.
54. IWM. *Environmental and Social Assessment (ESA), Bangladesh Economic Zones Authority (BEZA), Final Report*; IWM: Dhaka, Bangladesh, 2020.
55. Bangladesh Bureau of Statistics. *Population and Housing Census 2011*; Bangladesh Bureau of Statistics: Dhaka, Bangladesh, 2011.
56. Chadha, D.K. A Proposed New Diagram for Geochemical Classification of Natural Waters and Interpretation of Chemical Data. *Hydrogeol. J.* **1999**, *7*, 431–439. [[CrossRef](#)]
57. Piper, A.M. A Graphic Procedure in the Geochemical Interpretation of Water-Analyses. *Trans. Am. Geophys. Union* **1944**, *25*, 914. [[CrossRef](#)]
58. Durov, S.A. Natural Waters and Graphical Representation of Their Composition: Doklady Akademii Nauk. *Union Sov. Social. Repub.* **1948**, *59*, 87–90.
59. Horton, R.K. An Index Number System for Rating Water Quality. *J. Water Pollut. Control Fed.* **1965**, *37*, 300–306.
60. Saeedi, M.; Abessi, O.; Sharifi, F.; Meraji, H. Development of Groundwater Quality Index. *Environ. Monit. Assess.* **2010**, *163*, 327–335. [[CrossRef](#)]
61. Tyagi, S.; Sharma, B.; Singh, P.; Dobhal, R. Water Quality Assessment in Terms of Water Quality Index. *Am. J. Water Resour.* **2013**, *1*, 34–38. [[CrossRef](#)]
62. Packialakshmi, S.; Deb, M.; Chakraborty, H. Assessment of Groundwater Quality Index in and around Sholinganallur Area, Tamil Nadu. *Indian J. Sci. Technol.* **2015**, *8*, 1–7. [[CrossRef](#)]
63. Rezaei, A.; Hassani, H.; Tziritis, E.; Fard Mousavi, S.B.; Jabbari, N. Hydrochemical Characterization and Evaluation of Groundwater Quality in Dalgan Basin, SE Iran. *Groundw. Sustain. Dev.* **2020**, *10*, 100353. [[CrossRef](#)]
64. Richards, L.A. *Diagnosis and Improvement of Saline and Alkali Soils*; Agriculture Handbook No 60; United States Salinity Laboratory, US Department of Agriculture: Washington, DC, USA, 1954.
65. Wilcox, L. *Classification and Use of Irrigation Waters*; No. 969; US Department of Agriculture: Washington, DC, USA, 1955.
66. Bauder, J.W.; Brock, T.A. Irrigation Water Quality, Soil Amendment, and Crop Effects on Sodium Leaching. *Arid L. Res. Manag.* **2001**, *15*, 101–113. [[CrossRef](#)]
67. Post, V.E.A.; Groen, J.; Kooi, H.; Person, M.; Ge, S.; Edmunds, W.M. Offshore Fresh Groundwater Reserves as a Global Phenomenon. *Nature* **2013**, *504*, 71–78. [[CrossRef](#)] [[PubMed](#)]
68. Michael, H.A.; Scott, K.C.; Koneshloo, M.; Yu, X.; Khan, M.R.; Li, K. Geologic Influence on Groundwater Salinity Drives Large Seawater Circulation through the Continental Shelf. *Geophys. Res. Lett.* **2016**, *43*. [[CrossRef](#)]
69. BGS; DPHE. *Arsenic Contamination of Groundwater in Bangladesh*; British Geological Survey Technical Report WC/00/19; British Geological Survey: Nottingham, UK, 2001; Volume 4, pp. 22–31.

70. Rahman, M.; Tokunaga, T.; Yamanaka, T. Origin and Evolutionary Processes of Deep Groundwater Salinity in Southwestern Coastal Region of the Ganges-Brahmaputra-Meghna Delta, Bangladesh. *J. Hydrol. Reg. Stud.* **2021**, *36*, 100854. [[CrossRef](#)]
71. World Bank. *Implications of Climate Change for Fresh Groundwater Resources in Coastal Aquifers in Bangladesh*; World Bank: Washington, DC, USA, 2010.
72. Khan, M.R. Groundwater Chemistry of Mirsharai Upazila Chattogram, HydroShare. 2022. Available online: <http://www.hydroshare.org/resource/ce9529d9678e4f988739aab517acf1b2> (accessed on 5 June 2022).